



AD-A166 520

AD

TECHNICAL REPORT BRL-TR-2718

AN EXPERIMENTAL INVESTIGATION OF
THE ROLE OF SHEAR IN INITIATION
OF DETONATION BY IMPACT

Philip M. Howe
Gould Gibbons, Jr.
Patricia E. Webber

March 1986

DTIC
ELECTE
APR 15 1986
S
A
D

DTIC FILE COPY

APPROVED FOR PUBLIC RELEASE; DISTRIBUTION UNLIMITED.

US ARMY BALLISTIC RESEARCH LABORATORY
ABERDEEN PROVING GROUND, MARYLAND

86 4 15 114

Destroy this report when it is no longer needed.
Do not return it to the originator.

Additional copies of this report may be obtained
from the National Technical Information Service,
U. S. Department of Commerce, Springfield, Virginia
22161.

The findings in this report are not to be construed as an official
Department of the Army position, unless so designated by other
authorized documents.

The use of trade names or manufacturers' names in this report
does not constitute indorsement of any commercial product.

REPORT DOCUMENTATION PAGE		READ INSTRUCTIONS BEFORE COMPLETING FORM
1. REPORT NUMBER Technical Report BRL-TR-2718	2. GOVT ACCESSION NO. AD-A166520	3. RECIPIENT'S CATALOG NUMBER
4. TITLE (and Subtitle) AN EXPERIMENTAL INVESTIGATION OF THE ROLE OF SHEAR IN INITIATION OF DETONATION BY IMPACT.		5. TYPE OF REPORT & PERIOD COVERED
7. AUTHOR(s) PHILIP M. HOWE GOULD GIBBONS, JR. PATRICIA E. WEBBER		6. PERFORMING ORG. REPORT NUMBER
9. PERFORMING ORGANIZATION NAME AND ADDRESS US Army Ballistic Research Laboratory ATTN: SLCBR-TB Aberdeen Proving Ground, MD 21005-5066		8. CONTRACT OR GRANT NUMBER(s)
11. CONTROLLING OFFICE NAME AND ADDRESS US Army Ballistic Research Laboratory ATTN: SLCBR-DD-T Aberdeen Proving Ground, MD 21005-5066		10. PROGRAM ELEMENT, PROJECT, TASK AREA & WORK UNIT NUMBERS 1L161102AH43
14. MONITORING AGENCY NAME & ADDRESS (if different from Controlling Office)		12. REPORT DATE March 1986
		13. NUMBER OF PAGES 28
		15. SECURITY CLASS. (of this report) UNCLASSIFIED
16. DISTRIBUTION STATEMENT (of this Report) Approved for public release, distribution unlimited.		15a. DECLASSIFICATION DOWNGRADING SCHEDULE
17. DISTRIBUTION STATEMENT (of the abstract entered in Block 20, if different from Report)		
18. SUPPLEMENTARY NOTES COVER		
19. KEY WORDS (Continue on reverse side if necessary and identify by block number) Explosives Sensitivity, Impact Initiation, Shear Banding. — (containing shell)		
20. ABSTRACT (Continue on reverse side if necessary and identify by block number) Heavily confined explosive targets were subjected to impacts by explosively launched plates and by penetrating fragments. In each experiment, the damaged explosive was collected, sectioned, and examined by optical and scanning electron microscopy. A number of different types of damage was observed, each of which is expected to contribute to the initiation process. The response of the explosive to impacts is more complicated than originally thought. Since the explosive is mechanically weak, the conditions for shear damage are almost entirely controlled		

20. ABSTRACT (continued) . . .

by casing response to the impact, and the domain over which severe damage occurs is controlled by case deformation. We are as yet unable to rank these various explosive damage mechanisms with respect to their importance to the initiation process. *Keywords:*

to 5-10-19

ACKNOWLEDGEMENTS

The authors are grateful to Mr. Jerry Watson for many helpful discussions.

TABLE OF CONTENTS

	Page
LIST OF ILLUSTRATIONS	7
I. INTRODUCTION	9
II. EXPERIMENTAL	9
III. RESULTS AND DISCUSSION	13
IV. SUMMARY	20
LIST OF REFERENCES	23
DISTRIBUTION LIST	25

Accession For	
NTIS CRA&I	<input checked="" type="checkbox"/>
DTIC TAB	<input type="checkbox"/>
Unannounced	<input type="checkbox"/>
Justification _____	
By _____	
Distribution / _____	
Availability Codes	
Dist	Avail and/or Special
A-1	



LIST OF ILLUSTRATIONS

Figure

1	Schematic of Test Setup for Plate Impact Experiments	10
2	Test Projectile, Sectioned After Impact. Section was Obtained from the Center of the Impacted Region	11
3	Cylindrical Cross Section of Impacted Target. Corings were Removed for Microscopic Examination. Top View	11
4	Bottom View of Cross Section of Impacted Sample. Compare with Figure 3; Note Difference in Deformation and Blackened Region	14
5	Cross Section of Round, Showing Major Shear Cracks and Regions of High Damage	14
6	Close up View of Blackened Region. Blackening is a Result of Chemical Decomposition	15
7	Blackened Region at Higher Magnification. Note Boundary Between Case and Blackened Region	15
8	Microphoto of Major Shear Crack in TNT. Darkened Region at End of Crack is a Result of Powdered Explosive Removed from Sample During Polishing	17
9a	Optical Micrograph of Major Crack, Showing Fracture Damage and Some Internal Healing (Plane Polarized Light)	17
9b	Same Region of Crack as in 9a, Viewed with Partially Polarized Light. Note Outline of Grain Boundaries	18
9c	Crack Region of 9a Viewed with Reflected Light. Note High Degree of Flow, Grain Damage in Crack Region	18
10	Major Shear Crack Showing Region of Very Narrow Crack Width . . .	19
11	Collage Made from Figure 10 Showing Extent of Slip Along Crack .	19
12	Micrograph Showing Impact-Induced Slip and Grain Boundary Damage	21
13	Unimpacted Sample Showing Slip	21
14	Micrograph of Major Shear Crack Region in Impacted Composition B. Most of Shear Occurs in TNT Phase	21

I. INTRODUCTION

In recent years, numerous investigators have proposed different hot spot initiation models for the impact initiation of detonation. Field, et al¹ have shown that catastrophic shear failures can cause ignition, even if the catastrophic shear failures occur in inert plastics rather than in the explosive. They have also shown that crack propagation, by itself, is insufficient for ignition, but have speculated that the crack generation is sensitizing. Coffey² has proposed that dislocation pile up within crystals can cause shear banding, which in turn can lead to ignition. Mader³ has used a hydrodynamic hot spot model to describe initiation and has stated that the hydrodynamic hot spot model is all that is required to model ignition and buildup to detonation, for higher pressure (~10 kbar) shock initiation of heterogeneous explosives.⁴ Cavity collapse processes have been modelled by Frey,⁵ using an extension of the model of Carroll and Holt.⁶ In the range of pressures of interest to Frey, the hydrodynamic heating processes treated by Mader were less important than plastic work and shear processes.

Most of these models were developed without access to experimental results under conditions of interest. In particular, very little experimental work has been published describing the various damage forms arising from impacts upon explosives under heavily confined conditions. Furthermore, given that a multiplicity of phenomena could contribute to the initiation process, it becomes important to identify which ones provide the most significant contributions. The experimental work described herein represents a first attempt at characterizing the material response processes which occur within heavily confined explosive charges subjected to impact.

II. EXPERIMENTAL

Samples of heavily confined explosive charges were impacted by flying steel plates. Two types of TNT loaded projectiles were impacted, creamed and not creamed. The term "creamed", refers to a process whereby TNT powder is added to the molten batch of TNT during the hot melt casting procedure. The addition of the powder provides a large number of nucleation sites, and induces small crystal growth.

The 76 mm x 152 mm x 6 mm mild steel plates were explosively driven by Dupont Deta Sheet, and were thrown at 340 and 440 m/sec. The impacted rounds were prevented from hitting the wall of the firing site barbette by the use of sand bags. The different plate velocities provided different initial shocks, and different rates of projectile deformation. There were two variables functioning in the test configuration, plate velocity and TNT grain size. Fig. 1 is typical of the test setup in this firing program.

Control samples (not impacted) were kept from each lot, to be used as undamaged standards in the microstructural study of the impacted explosives.

Both the control and impacted projectiles were remotely cut, and cylindrical sections were removed for microscopic investigation. No fluids were used in the cutting process so as to minimize the probability of contamination. The sections taken were approximately 50 mm thick. Fig. 2 represents a typical cut projectile, and Fig. 3 shows a cylindrical section.

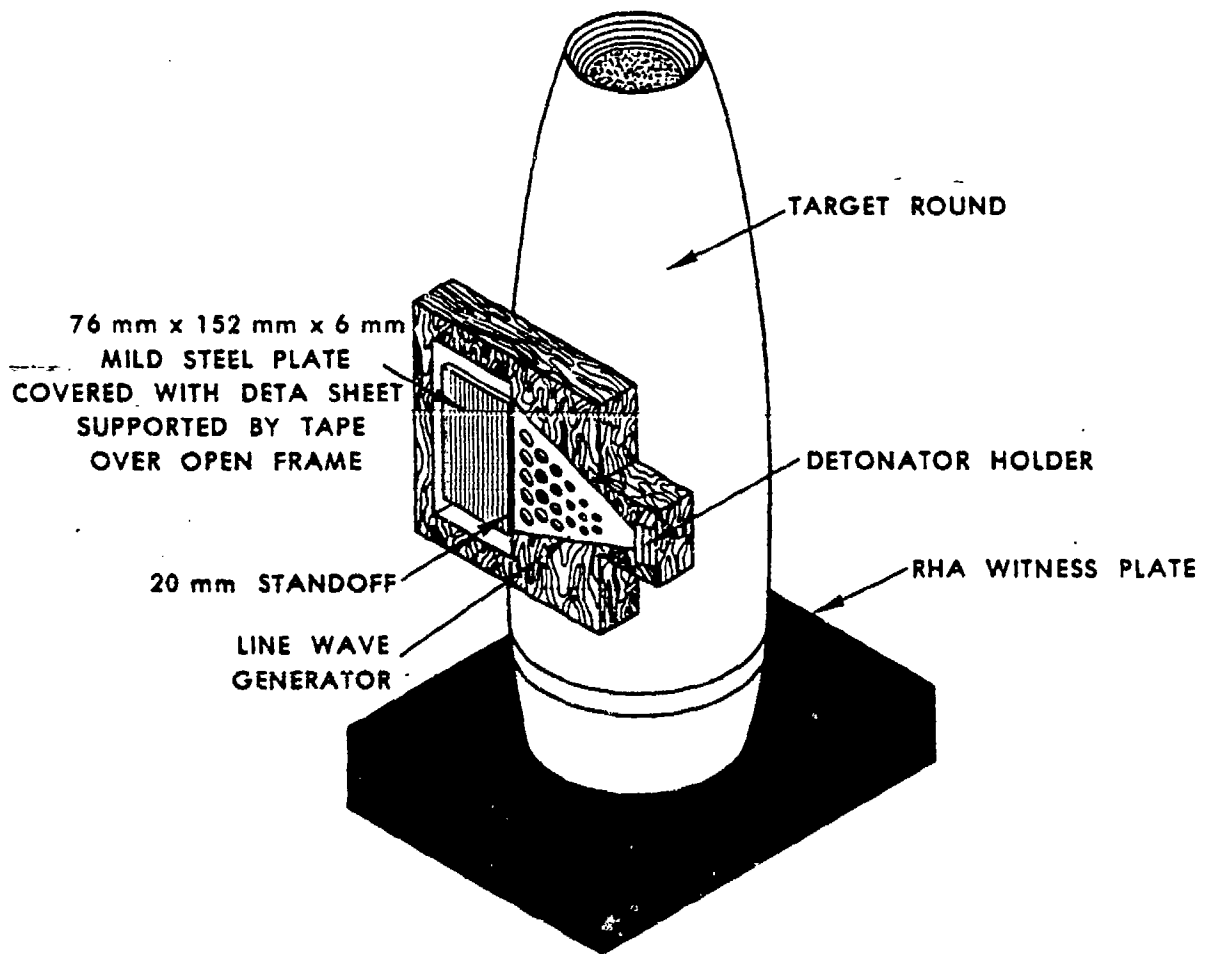


Figure 1. Schematic of Test Setup for Plate Impact Experiments.

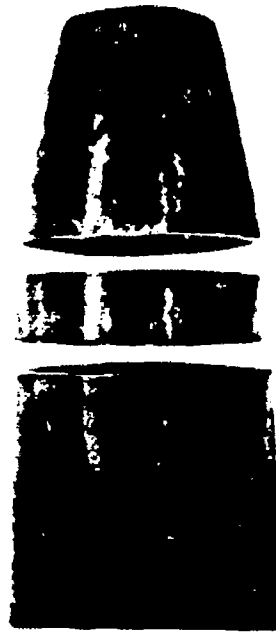


Figure 2. Test Projectile, Sectioned After Impact. Section was Obtained From the Center of the Impacted Region.

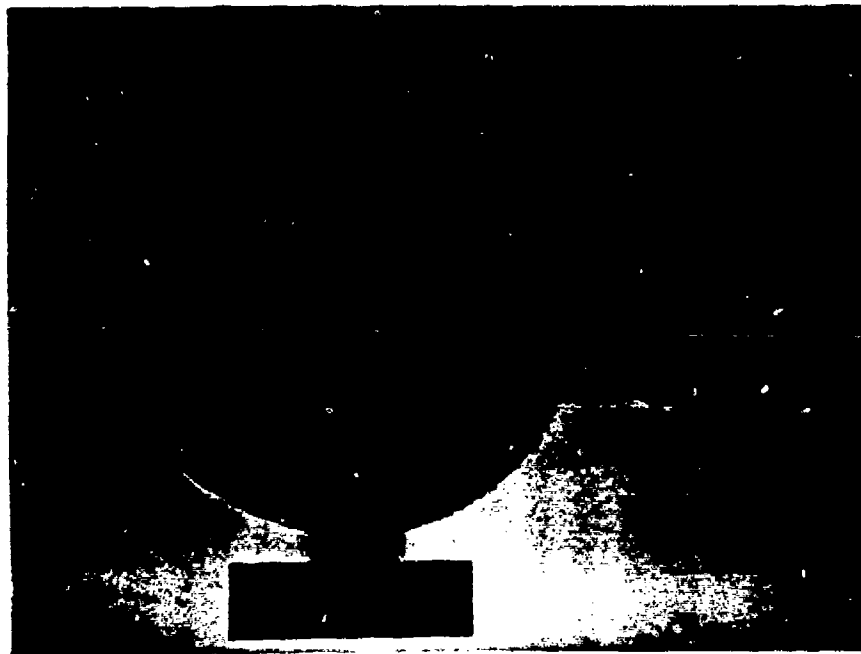


Figure 3. Cylindrical Cross Section of Impacted Target. Corings were removed for Microscopic Examination. Top View.

Sample corings were removed from various locations within the sections taken from the cut rounds. The corings were removed by hand, using a standard hole saw; no power equipment was used at this point in the sample preparation. The samples were sanded flat on one side, so that the flat was parallel to the plate impact; this flat provides an orientation landmark for the direction of the impact. The original cut surface (made when the round was sectioned), and a plane parallel to the cut surface, were coarse sanded using 150 grit sandpaper followed by 320 grit sandpaper. The flat opposite the cut surface was glued to an aluminum SEM sample stud using a silver base acrylic paint.

The surface to be investigated was again sanded in final preparation for polishing using 150 and 320 grit sandpaper, and then fine sanded using 400 and 600 grit sandpaper. All sanding was done by hand, without water. An effort was made to keep the prepared surface perpendicular to the axis of the mounting stud, and obtain a smooth 600 grit finish.

After sanding, the sample was hand polished using a wool polishing cloth saturated with distilled water. The wool cloth was manufactured by Buehler, Ltd.. The Buehler cloth was cataloged as, "AB Kitten Ear", no. 40-7556. This material has been discontinued by Buehler, but can be purchased from:

J.I. Morris Company
394 Elm Street
P.O. Box 70
Southbridge, Mass. 01550

Phone: (617) 764-4394

Item: U-18 Pressed Wool Pad

The sample being polished was rinsed with distilled water, and dried with compressed Freon. Polishing was done with a light pressure, while moving the sample in a figure eight motion.

Optical microscopic examinations were done using an Optiphot Microscope by Nikon. Two types of surface lighting were used; polarized light, and normal or scattered light. Normal lighting provides the best delineation of the TNT grains; but both types of light have their advantages, each providing different data. A partially polarized light source also proved useful.

Samples for scanning electron microscopic (SEM) examination were prepared by sputtering a conductive coating of gold, or gold/palladium onto the surface. The sputter coating for this work was done in a Denton Vacuum, Inc.; Desk 1; Sputter Unit. A gold/palladium coating was applied at an argon pressure of 75 mtorr, and a current of 15 mA for 2 minutes. These sputter conditions provide a conductive film thickness of about 500 angstroms. A film of this thickness has been found to be the minimum thickness suitable for SEM work on an explosive sample.

The sample can be chemically etched after polishing to enhance the TNT grain boundaries. It was found that 1,2 dichloroethane is an excellent solvent for etching TNT. This chemical is toxic and was not allowed to come in contact with skin, nor were the vapors inhaled. Etching was completed by dipping the sample in fresh stirring solvent, for 3 seconds. Dissolution was quenched

after 3 seconds by immediate immersion in distilled water. The samples were rinsed with distilled water, and dried with compressed Freon. Pure solvent was used for each sample so that the rate of dissolution was constant from sample to sample. Mild stirring was effected by using a magnetic stirrer.

III. RESULTS AND DISCUSSION

Examination of sections of artillery shell subjected to impacts by explosively launched plates revealed several phenomena which appear to be important to the initiation process. The intensity with which these phenomena occurs is an increasing function of severity of impact.

Shown in Fig. 3 and 4 is a cross sectional view of a target round, which had been impacted at 440 m/s by a 0.64 cm steel plate. Near the point of impact is a kidney bean shaped area which has been severely damaged. Grains have been comminuted, and intergranular separation has occurred. The blackened regions are localized areas of decomposition. Chemical analysis indicates that the decomposition is rather complete; the main product identified as being present was carbon.* Microscopic examination of these blackened regions revealed two morphologies, as shown in Fig. 5 and in the microphotos of Fig. 6 and 7. One family of blackened regions appears as relatively long, narrow region oriented parallel to lines of principal shear, and is probably an example of shear-induced hot spot formation. Note that these regions occur at grain boundaries and as shear failures within individual grains. The second family of blackened regions is more spherical in nature, has no preferred orientation, and quite probably is a result of cavity collapse processes. Note that, in this particular sample, the number density of shear-induced hot spots is greater than that of cavity collapse-induced hot spots, although both are present. The proportion will be a function of sample porosity and deviations from planar, uniaxial flow.

Between the bean-shaped region of high damage and the warhead casing is a narrow band showing little damage (see Fig. 3). This band is reproducible from shot to shot. Apparently, it was caused by heat conduction to the steel casing. If this is true, it indicates that the decomposition within the region of high damage was a relatively slow process.

* In the region of severe blackening, directly behind the impact point, decomposition of TNT was confirmed by chemical analysis. The black material was found to be carbon. Surface analysis, via X-Ray Photoelectron Spectroscopy (XPS), indicated the possible presence of oxidation products of TNT. Peak broadening in the XPS spectra indicated the presence of the acid or aldehyde derivative, and also the possibly of a nitrile derivative. TLC was used to further evaluate the sample, and four compounds were identified. TLC comparison with reference compounds, and mass spectra confirmed the four compounds as TNT; 2, 4, 6 trinitrobenzaldehyde; 2, 4, 6 trinitrobenzoxime; and 2, 4, 6 trinitrobenzoxime. The oxime is a second step decomposition product, in that it probably results from the reaction of trinitrobenzyl anion with nitrous acid. The nitrile is then formed by dehydration of the oxime. These results are consistent with a rather complete, localized decomposition of the TNT. (Private communication with J. Sharma; Naval Surface Weapons Center, White Oak, Silver Spring, MD 20910)



Figure 4. Bottom View of Cross Section of Impacted Sample. Compare with Figure 3; Note Difference in Deformation and Blackened Region.

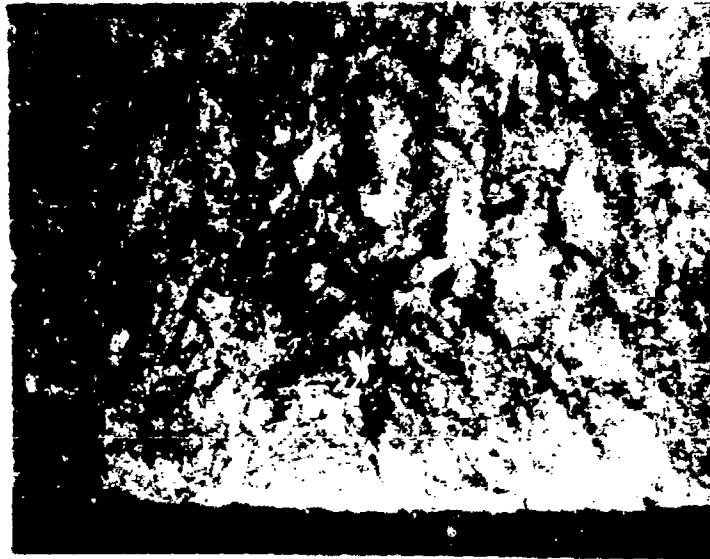


Figure 5. Cross Section of Round, Showing Major Shear Cracks and Regions of High Damage.



1 mm

Figure 6. Close up View of Blackened Region. Blackening is a Result of Chemical Decomposition.



1 mm

Figure 7. Blackened Region at Higher Magnification. Note Boundary Between Case and Blackened Region.

The volume of the bean-shaped region of high damage correlates with case deformation. For similar impact geometries, higher impact velocities produced larger damaged volumes, and greater density of decomposed regions within these volumes. Where case thickness variations cause different deformations, the damaged volume appears to scale with total deformation, and the density of hot spots within the damaged volume correlates with impact velocity. The fact that impacts in thinner cases yielded larger regions of high damage indicates that the damage was caused primarily by case deformation, not shock loading, as small changes in wall thickness would not cause appreciable differences in shock loading. To check this, computer calculations were conducted replicating the impact conditions. Results showed that the shock loading conditions are essentially the same for the two impact conditions.

Each of the impacted samples exhibited a field of major shear cracks, external to the regions of high damage, as shown in Fig. 3 and 4 and as shown in Fig. 5. The width of individual shear cracks was found to vary significantly and randomly across a sample. Cracks as wide as 0.1 mm and as narrow as 0.01 mm were observed. Microscopic examination of these cracks revealed several interesting features. In the wider regions, the explosive was severely shattered within the crack, to the point where integrity of the sample was lost, and polishing was difficult or impossible (see Fig. 8). In the narrower regions, cracking and comminution of the grains occurred, and melting and fusing occurred as well. In these regions, sample integrity was reestablished, and polishing was possible. One such area is shown in Fig. 9a through 9c. In Fig. 9a, partial melting is clearly apparent. Some fractures are apparent within the crack, but most have been healed. At the edges of the crack, many small fractures are apparent. These may have occurred after crack formation and healing, or they may have occurred during crack formation but, because they were at the edges of the crack, did not reach a high enough temperature to heal. Fig. 9a through 9c are photomicrographs of the same region, but with different lighting, to highlight different crack features. Figure 9a discussed above, was obtained with plane polarized light, to reduce surface reflections. Figure 9c was obtained with unpolarized light, to emphasize surface characteristics. Here, one can discuss the intersection of grain boundaries with the highly polished specimen surface. Note the large amount of flow which has occurred within the region. Healing of internal fractures has occurred, and partial melting has also occurred. Some discoloration within the crack was noted, indicating that partial decomposition may have occurred. Figure 9b was obtained with partially polarized light and permits comparison of 9a and 9c, having some features of each.

The majority of macroscopic shear cracks exhibit the features described above. Evidently, formation of these cracks involves local shear failures over a wide region, with shattering and grinding of the explosive occurring within the crack. If the motions and pressures are adequate, healing, melting, and decomposition can occur. Occasionally, macroscopic shear cracks can propagate with relatively little damage to the grain structure, and with little indication of decomposition or local heating. Such a crack is shown in Fig. 10. Note that, in one region, the crack width has narrowed to a dimension of the order of a grain boundary. Significant slip has occurred; Fig. 11 shows a collage made by cutting along the crack and matching grain boundaries. In this instance the total slip was ~ 0.04 mm.



Figure 8. Microphoto of Major Shear Crack in TNT. Darkened Region at End of Crack is a Result of Powdered Explosive Removed from Sample During Polishing.

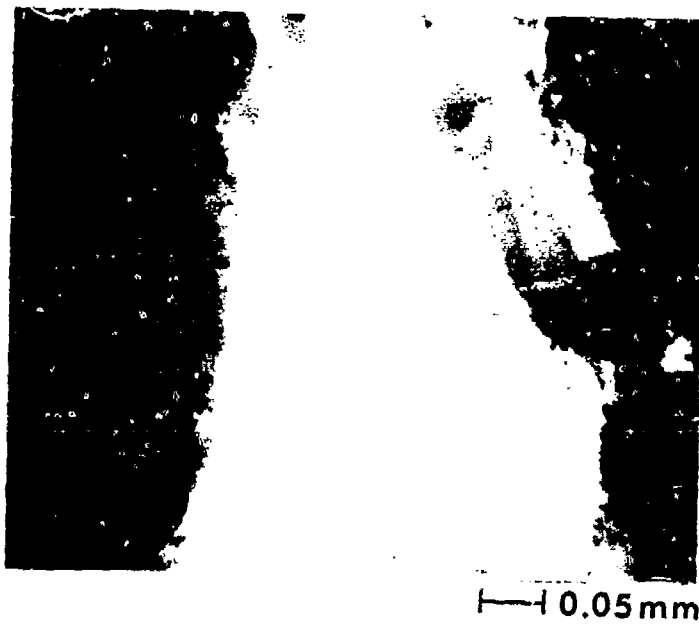
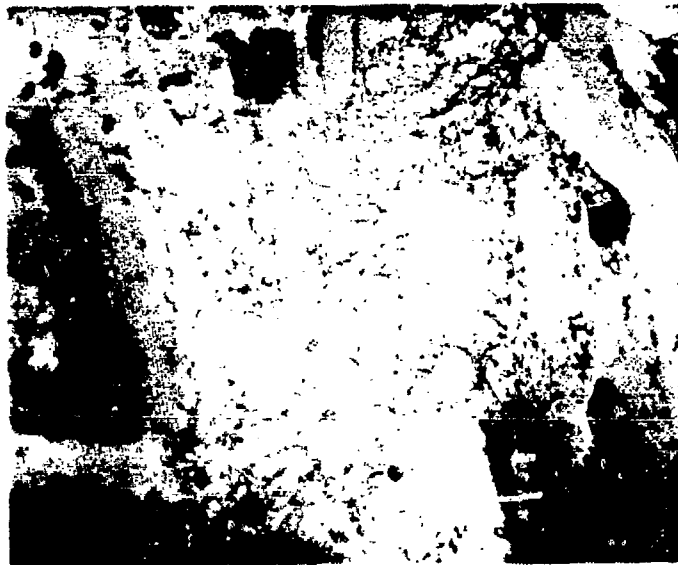


Figure 9a. Optical Micrograph of Major Crack, Showing Fracture Damage and Some Internal Healing (Plane Polarized Light).



—| 0.05 mm

Figure 9b. Same Region of Crack as in 9a, Viewed with Partially Polarized Light. Note Outline of Grain Boundaries.



—| 0.05 mm

Figure 9c. Crack Region of 9a Viewed with Reflected Light. Note High Degree of Flow, Grain Damage in Crack Region.



Figure 10. Major Shear Crack Showing Region of Very Narrow Crack Width.



Figure 11. Collage Made from Figure 10 Showing Extent of Slip Along Crack.

Between major shear cracks, damage is considerably less. Impact damage shows up in the form of internal fractures, separation at grain boundaries, and slip. Slip induced by impact is relatively easy to distinguish from slip bands formed during crystallization due to the former displaying crushed regions where slip bands meet grain boundaries. An example of incipient grain boundary separation and impact-induced slip is shown in Fig. 12. For comparison, an unimpacted sample is shown in Fig. 13. In regions distant from the point of impact, none of these damage forms showed any indication of melting or significant decomposition, as indicated by discoloration of the sample, and such mild damage probably does not contribute to ignition. However, it is quite likely that there would be a significant contribution to processes, such as grain burning, which are involved in the post-ignition buildup to detonation.

At a given impact velocity, damage was found to be more severe in the large grain size (uncreamed) TNT than in the fine grain size (creamed) samples. This difference is manifested most strongly in the region of high damage, near the point of impact, with the decomposition being much more extensive within the damaged volume, and the damaged volume much larger for the large grain sample.

Increases in impact velocity led to increased damage, as expected. Fracture damage throughout the impacted sample is more severe at the higher impact velocity, with much more extensive grain separation, internal fracture damage, slip, and macroscopic shear crack formation. At the higher impact velocity, the number of macroscopic shear cracks is greater, and the extent of melting is greater. Discoloration due to decomposition is much more extensive in these cracks. A more quantitative description must await examination of samples impacted at more than two velocities.

A few experiments were conducted using gun launched cylindrical projectiles which led to perforating impacts. The region of high damage observed in the plate impact experiments is replaced by cratering. Away from the crater, damage to the sample was very similar to that for the plate impact experiments. However, almost all the deformation occurred within the TNT phase, with the RDX relatively untouched. This is shown in Fig. 14, where the explosive was composition B (60% RDX, 40% TNT). Chemical analysis identified the presence of partial decomposition products of TNT, but not of RDX.

In addition to the internal damage, there is clear evidence of significant melting and flow away from the point of impact, between the explosive and the casing. How important this is to initiation is unknown.

IV. SUMMARY

Heavily confined explosive targets were subjected to impacts by explosively launched plates and by penetrating fragments. In each experiment, the damaged explosive was collected, sectioned, and examined by optical and scanning electron microscopy. A number of different types of damage was observed, each of which is expected to contribute to the initiation process. Near the point of impact, for non-perforating impacts, a severely damaged region was observed. This region showed evidence of decomposition of the explosive. The decomposition within this region was localized, and nearly complete; i.e., carbon was identified, but few intermediate decomposition products. Separating this region of high damage and decomposition from the casing was a thin layer of



Figure 12. Micrograph Showing Impact-Induced Slip and Grain Boundary Damage.



Figure 13. Unimpacted Sample Showing Slip.



Figure 14. Micrograph of Major Shear Crack Region in Impacted Composition B. Most of Shear Occurs in TNT Phase.

explosive, exhibiting no significant decomposition. This is probably a result of heat transfer to the casing, and indicates that the decomposition in this region at the impact conditions studied was rather slow.

Outside the region of high damage, the explosive exhibited families of major catastrophic shear cracks. The width of these cracks varied from ~ 0.01 mm to ~ 0.1 mm. Evidence of melting and decomposition was observed in the thinner regions of the cracks.

Results for impacts with perforating fragments were similar to those for plate impacts, except that cratering replaced the region of high damage. All the other phenomena were quite similar.

The response of the explosive to impacts is more complicated than originally thought. Since the explosive is mechanically weak, the conditions for shear damage are almost entirely controlled by casing response to the impact, and the domain over which severe damage occurs is controlled by case deformation. We are as yet unable to rank these various explosive damage mechanisms with respect to their importance to the initiation process.

REFERENCES

1. Field, J.E., Swallowe, G.M., Heavens, S.N., "Ignition Mechanisms of Explosives during Mechanical Deformation," Proc. R. Soc Lond. A382 231 (1982).
2. Coffey, C.S., Frankel, M.J., Liddiard, T.P., Jacobs, S.J., "Experimental Investigation of Hotspots Produced by High Rate Deformation and Shocks," Proc Seventh Symp (Int) on Detonation, pp. 970 (1981).
3. Mader, C., "Numerical Modeling of Detonation," Los Alamos Series in Basic and Applied Sciences, U of C. Press, Berkeley, (1979).
4. Mader, C., "Invited Discussions of Shock Initiation Mechanism," Proc. Sixth Symp (Int) on Detonation, pp. 89 (1976).
5. Frey, R.B., "Cavity Collapse in Energetic Materials," Proceedings, this symposium.
6. Carroll, M.M., Holt, A.C., "Static and Dynamic Pore Collapse Relations for Ductile Porous Materials," J Applied Phys. 43, No. 4 (1972).

DISTRIBUTION LIST

<u>No. of</u> <u>Copies</u>	<u>Organization</u>	<u>No. of</u> <u>Copies</u>	<u>Organization</u>
12	Administrator Defense Technical Info Center ATTN: DTIC-DDA Cameron Station Alexandria, VA 22304-6145	1	Commander Armament R&D Center US Army AMCCOM ATTN: SMCAR-LCE, Dr. N. Slagg Dover, NJ 07801-5001
1	HQDA DAMA-ART-M Washington, DC 20310	1	Commander Armament R&D Center US Army AMCCOM ATTN: SMCAR-LCN, Dr. P. Harris Dover, NJ 07801-5001
1	Chairman DOD Explosives Safety Board ATTN: Dr. T. Z. r Room 856-C Hoffman Bldg 1 2461 Eisenhower Avenue Alexandria, VA 22331	1	Commander US Army Armament, Munitions and Chemical Command ATTN: SMCAR-ESP-L Rock Island, IL 61299
1	Chairman DOD Explosives Safety Board ATTN: COL O. Westry Room 856-C Hoffman Bldg 1 2461 Eisenhower Avenue Alexandria, VA 22331	1	Director Benet Weapons Laboratory US Army AMCCOM-ARDC ATTN: SMCAR-LCB-TL Watervliet, NY 12189
1	Commander U.S. Army Materiel Command ATTN: AMCDRA-ST 5001 Eisenhower Avenue Alexandria, VA 22333-0001	1	Commander US Army Aviation Research and Development Command ATTN: AMSAV-E 4300 Goodfellow Boulevard St. Louis, MO 63120
1	Commander Armament R&D Center US Army AMCCOM ATTN: SMCAR-TSS Dover, NJ 07801-5001	1	Director US Army Air Mobility Research and Development Laboratory Ames Research Center Moffett Field, CA 94035
1	Commander Armament R&D Center US Army AMCCOM ATTN: SMCAR-LCE, Dr. R. F. Walker Dover, NJ 07801-5001	1	Commander US Army Communications Electronics Command ATTN: AMSEL-ED Fort Monmouth, NJ 07703

DISTRIBUTION LIST

<u>No. of</u> <u>Copies</u>	<u>Organization</u>	<u>No. of</u> <u>Copies</u>	<u>Organization</u>
1	Commander ERADCOM Technical Library ATTN: DELSD-1 (Reports Section) Fort Monmouth, NJ 07703-5301	1	Commander US Army Research Office ATTN: Chemistry Division P.O. Box 12211 Research Triangle Park, NC 27709-2211
1	Commander, U.S. Army Missile Command Research, Development & Engineering Center, ATTN: AMSMI-RD Redstone Arsenal, AL 35898	1	Office of Naval Research ATTN: Dr. J. Enig, Code 200B 800 N. Quincy Street Arlington, VA 22217
1	Director U.S. Army Missile & Space Intelligence Center ATTN: ALAMS-YDL Redstone Arsenal, AL 35898-5500	1	Commander Naval Sea Systems Command ATTN: Mr. R. Beauregard, SEA 64E Washington, DC 20362
1	Commander US Army Missile Command ATTN: AMSME-RK, Dr. R.G. Rhoades Redstone Arsenal, AL 35898	1	Commander Naval Explosive Ordnance Disposal Technology Center ATTN: Technical Library Code 604 Indian Head, MD 20640
1	Commander US Army Tank Automotive Command ATTN: AMSTA-TSL Warren, MI 48397-5000	1	Commander Naval Research Lab ATTN: Code 6100 Washington, DC 20375
1	Director US Army TRADOC Systems Analysis Activity ATTN: ATAA-SL White Sands Missile Range NM 88002	1	Commander Naval Surface Weapons Center ATTN: Code G13 Dahlgren, VA 22448
1	Commandant US Army Infantry School ATTN: ATSH-CD-CSO-OR Fort Benning, GA 31905	1	Commander Naval Surface Weapons Center ATTN: Mr. L. Roslund, R122 Silver Spring, MD 20910
1	Commander US Army Development & Employment Agency ATTN: MODE-TED-SAB Fort Lewis, WA 98433	1	Commander Naval Surface Weapons Center ATTN: Mr. M. Stosz, R121 Silver Spring, MD 20910
		1	Commander Naval Surface Weapons Center ATTN: Code X211, Lib Silver Spring, MD 20910

DISTRIBUTION LIST

<u>No. of</u> <u>Copies</u>	<u>Organization</u>	<u>No. of</u> <u>Copies</u>	<u>Organization</u>
1	Commander Naval Surface Weapons Center ATTN: E. Zimet, R13 Silver Spring, MD 20910	1	Commander Naval Weapons Center ATTN: Dr. K.J. Graham, Code 3835 China Lake, CA 93555
1	Commander Naval Surface Weapons Center ATTN: R.R. Bernecker, R13 Silver Spring, MD 20910	1	Commander Naval Weapons Station NEDED ATTN: Dr. Louis Rothstein, Code 50 Yorktown, VA 23691
1	Commander Naval Surface Weapons Center ATTN: J.W. Forbes, R13 Silver Spring, MD 20910	1	Commander Fleet Marine Force, Atlantic ATTN: G-4 (NSAP) Norfolk, VA 23511
1	Commander Naval Surface Weapons Center ATTN: S.J. Jacobs, R10 Silver Spring, MD 20910	1	Commander Air Force Rocket Propulsion Laboratory ATTN: Mr. R. Geisler, Code AFRPL MKPA Edwards AFB, CA 93523
1	Commander Naval Surface Weapons Center ATTN: Dr. C. Dickinson Silver Spring, MD 20910	1	AFWL/SUL Kirtland AFB, NM 87117
1	Commander Naval Surface Weapons Center ATTN: J. Short, R12 Silver Spring, MD 20910	1	Air Force Armament Laboratory ATTN: AFATL/DLODL Eglin AFB, FL 32542-5000
1	Commander Naval Weapons Center ATTN: Dr. L. Smith, Code 3205 China Lake, CA 93555	1	Commander Ballistic Missile Defense Advanced Technology Center ATTN: Dr. David C. Sayles P.O. Box 1500 Huntsville, AL 35807
1	Commander Naval Weapons Center ATTN: Dr. A. Amster, Code 385 China Lake, CA 93555	1	Director Lawrence Livermore National Lab University of California ATTN: Dr. M. Finger P.O. Box 808 Livermore, CA 94550
1	Commander Naval Weapons Center ATTN: Dr. R. Reed, Jr., Code 388 China Lake, CA 93555	1	Director Los Alamos National Lab ATTN: John Ramsey P.O. Box 1663 Los Alamos, NM 87545

DISTRIBUTION LIST

<u>No. of Copies</u>	<u>Organization</u>	<u>No. of Copies</u>	<u>Organization</u>
1	Director Sandia National Lab ATTN: Dr. J. Kennedy Albuquerque, NM 87115	1	Commander Armament R&D Center U.S. Army AMCCOM ATTN: SMCAR-TDC Dover, NJ 07801
	<u>Aberdeen Proving Ground</u>	10	Central Intelligence Agency Office of Central Reference Dissemination Branch Room GE-47 HQS Washington, D.C. 20502
	Dir, USAMSAA ATTN: AMXSU-D AMXSU-MP, H. Cohen		
	Cdr, USATECOM ATTN: AMSTE-TO-F		
	Cdr, CRDC, AMCCOM, ATTN: SMCCR-RSP-A SMCCR-MU SMCCR-SPS-IL		

USER EVALUATION SHEET/CHANGE OF ADDRESS

This Laboratory undertakes a continuing effort to improve the quality of the reports it publishes. Your comments/answers to the items/questions below will aid us in our efforts.

1. BRL Report Number _____ Date of Report _____

2. Date Report Received _____

3. Does this report satisfy a need? (Comment on purpose, related project, or other area of interest for which the report will be used.) _____

4. How specifically, is the report being used? (Information source, design data, procedure, source of ideas, etc.) _____

5. Has the information in this report led to any quantitative savings as far as man-hours or dollars saved, operating costs avoided or efficiencies achieved, etc? If so, please elaborate. _____

6. General Comments. What do you think should be changed to improve future reports? (Indicate changes to organization, technical content, format, etc.) _____

CURRENT
ADDRESS

Name

Organization

Address

City, State, Zip

7. If indicating a Change of Address or Address Correction, please provide the New or Correct Address in Block 6 above and the Old or Incorrect address below.

OLD
ADDRESS

Name

Organization

Address

City, State, Zip

(Remove this sheet along the perforation, fold as indicated, staple or tape closed, and mail.)

FOLD HERE

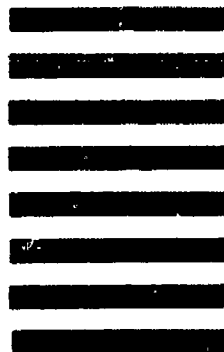
Director
U.S. Army Ballistic Research Laboratory
ATTN: SLCBR-DD-T
Aberdeen Proving Ground, MD 21005-5066



NO POSTAGE
NECESSARY
IF MAILED
IN THE
UNITED STATES

OFFICIAL BUSINESS
PENALTY FOR PRIVATE USE, \$300

BUSINESS REPLY MAIL
FIRST CLASS PERMIT NO 12062 WASHINGTON, DC
POSTAGE WILL BE PAID BY DEPARTMENT OF THE ARMY



Director
U.S. Army Ballistic Research Laboratory
ATTN: SLCBR-DD-T
Aberdeen Proving Ground, MD 21005-9989

FOLD HERE